Journal Name RSCPublishing

ARTICLE

Reactivity of copper-α-synuclein peptide complexes relevant to Parkinson's disease

Cite this: DOI: 10.1039/x0xx00000x

Received 00th January 2012, Accepted 00th January 2012

DOI: 10.1039/x0xx00000x

www.rsc.org/

Simone Dell'Acqua,[a]* Valentina Pirota,[a] Cecilia Anzani,[a] Michela M. Rocco,[a] Stefania Nicolis,[a] Daniela Valensin,[b] Enrico Monzani,[a] and Luigi Casella[a]*

Parkinson's disease (PD) is a neurodegenerative disorder characterized by the presence of abnormal α-synuclein (αSyn) deposits in the brain. Alterations in metal homeostasis and metal-induced oxidative stress may play a crucial role in the aggregation of αSyn and, consequently, in the pathogenesis of PD. We have therefore investigated the capability of copper-αSyn6 and copper-αSyn15 peptide complexes, with the 1-6 and 1-15 terminal fragments of the protein, to promote redox reactions that can be harmful to other cellular components. The pseudo-tyrosinase activity of copper-αSyn complexes against catecholic (di-*tert*-buthylcatechol ($DTBCH_2$) and 4-methylcatechol (4-MC) and phenolic (phenol) substrates is lower compared to that of free copper(II). In particular, the rates (k_{cat}) of $DTBCH_2$ catalytic oxidation are 0.030 s^{-1} and 0.009 s^{-1} for the reaction promoted by free copper(II) and [Cu^{2+}-αSyn15], respectively. On the other hand, HPLC/ESI-MS analysis of solutions of αSyn15 incubated with copper(II) and 4-MC showed that αSyn is competitively oxidized with remarkable formation of sulfoxide at Met1 and Met5 residues. Moreover, sulfoxidation of methionine residues, which is related to the aggregation of αSyn, also occurs on peptide not directly bound to copper, indicating that external αSyn can also be oxidized by copper. Therefore, this study strengthens the hypothesis that copper plays an important role in oxidative damage of αSyn which is proposed to be strongly related to the etiology of PD.

Introduction

Alpha-synuclein (αSyn) is a highly soluble, intrinsically disordered protein of 140 residues, localized at presynaptic terminals in close proximity to synaptic vesicles.[1] The physiological role of αSyn has been related to membrane binding, synaptic vesicle recycling,[2] and dopamine metabolism.[3, 4] The formation of αSyn prefibrillar oligomers has been associated with neurodegeneration in Parkinson's disease (PD).[5-7] The first evidence of αSyn neurotoxicity is the presence of intracellular inclusions called Lewy bodies that consist in aggregates of this protein.[7] The mechanism of formation and assembly of protein aggregates is complex and still object of several studies, but there is increasing evidence that breakdown in metal homeostasis is crucial in different age-related neurodegenerative diseases.[8, 9]

Several metal ions can bind αSyn, but only copper(II) can bind αSyn in the micromolar range,[10] indicating a high affinity for Cu^{2+} of this protein. Moreover, copper(II)-αSyn interaction can enhance formation of amyloid fibrils.[11, 12] Copper(II) binding to αSyn has been therefore exhaustively investigated, showing the presence of two binding sites in the N-terminal region, "Site 1" and "Site 2".[10] In Site 1 copper is coordinated by the NH_2 group of Met1, the deprotonated amide of Asp2, the carboxylate side-chain of Asp2 and a water-derived ligand;[13, 14] in Site 2 copper is coordinated by the imidazole nitrogen of His50, deprotonated amide of His50 and Val49, and a water molecule.[12, 15] Dissociation constants show that Site 1 (K_d from 10^{-7} to 10^{-10} M)[14, 16-19] has higher affinity for Cu^{2+} compared to Site 2 (K_d from 10^{-5} to 10^{-6} M),[14] although some discrepancy in literature data exists, probably due to the use of different techniques for K_d determination. Furthermore, recent studies suggest the acetylation of αSyn *in vivo*,[20, 21] which implies that the copper(II) binding site anchored to Met1 amine group is abolished.[22]

Another copper-dependent mechanism for αSyn aggregation is related to the redox chemistry of this metal and the generation of reactive oxygen species (ROS) which lead to a cascade of structural alterations, such as site-specific oxidation, dityrosine cross-linking, protein truncation, that enhance αSyn aggregation.[10] These modifications of αSyn are important because they are prominent phenomena observed in post-mortem PD brain sections.[23] Oxidative modifications can affect αSyn aggregation,[24] as well as its interaction with biological membranes.[25] For these reasons, the attention of several studies has recently focused on the characterization of the redox chemistry of Cu^{2+}/Cu^{+}-αSyn complex. The redox potential spans from 0.217[26] to 0.371 V *vs.* SHE[27] for copper bound to full-length αSyn, while a redox potential of 0.252 V has been determined for the copper complex with the N-terminal portion of 1-19 residues.[26]

The binding of copper(I) to αSyn has also been studied by several techniques. NMR, CD and XAS spectroscopy,[28-30] and site-directed mutagenesis[31] demonstrate that Cu^+ can bind to two independent sites at the N- and C-terminal regions of αSyn, respectively, and in both cases two methionine sulfur atoms are involved in the metal coordination sphere. In the N-terminal site, which is more important due to the high-affinity for Cu^{2+}, Cu^+ is coordinated by the side chains of Met1, Asp2, Met5 and a water molecule, indicating that copper(II) and copper(I) binding sites are different and a structural rearrangement in the coordination sphere is required in reactions involving Cu^{2+}/Cu^+ redox change.

Despite the large number of investigations on the structural properties of copper-αSyn, little is known regarding the related reactivity. Lucas *et al*. investigated the redox properties of Cu^{2+}/Cu^+ bound to αSyn showing that Cu^{2+} can be reduced to Cu^+ in anaerobic conditions, whereas, in the presence of O_2, reoxidation of Cu^+ is associated to generation of ROS, which can promote dityrosine cross-linking.[32] Wang *et al.* showed that ascorbate reduces Cu^{2+}-αSyn to Cu^+-αSyn and that subsequent reoxidation by atmospheric oxygen leads to the formation of hydrogen peroxide, which exhibits a cytotoxic behavior.[26] Further studies indicated that Cu^{2+}-αSyn can promote dopamine oxidation, although the contribution of free copper to this reactivity was not investigated.[33] This study also showed that hydroxyl radicals are produced by Cu^{2+}-αSyn in the presence of ascorbate. Moreover, incubation of Cu^{2+}-αSyn with dopamine brings to methionine sulfoxidation.[34]

It is worth mentioning that another hypothesis regarding the relationship between copper homeostasis and PD pathogenesis relies on the observation that the total copper concentration in the pathogenic neurons affected by PD is decreased.[35] This observation and other studies showing the important role of copper in maintaining the cellular defence against superoxide through SOD1 system suggest that reduction of copper concentration in PD may reduce antioxidant defence and contribute to neurodegenerative cascades.[36]

An exhaustive study assessing the reactivity of Cu-αSyn species in crucial processes for the PD pathogenesis, such as ROS generation, αSyn modification, and the competitive oxidation of external substrates is therefore required. The latter issue is important because αSyn has been related to the metabolism of dopamine and the formation of copper-αSyn complex may interfere with this physiological regulation, since it is known that several copper-enzymes[37] or synthetic copper-complexes[38, 39] can catalyze catechol oxidation.

Herein, we aim at clarifying part of this complex frame by studying the reactivity of copper-αSyn complexes in the oxidation of catecholic and phenolic substrates, superoxide dismutation, and competitive endogenous modification of αSyn in the resulting oxidative environment. In particular, we have used N-terminal peptide fragments (αSyn15 and αSyn6) which contain the high affinity binding site of the protein[10, 28] and are, therefore, good models for mimicking copper-αSyn in both copper redox states.[13, 28]

Results and discussion

To gain information on the potential catalytic role of copper-αSyn15 and -αSyn6 complexes in oxidative reactions, we performed a detailed comparative study of their oxidative activity against catecholic and phenolic substrates with respect to that of free copper(II). The most important substrate that can be involved in this type of reactivity is dopamine, due to its high concentration in *substantia nigra* neurons and because alteration in dopamine metabolism, which appears to be regulated by αSyn, can be one of the causes of PD pathogenesis.[40] However, dopamine oxidation is a complex process because of the high reactivity of its primary product, dopaminoquinone, which leads to rapid formation of insoluble melanic products, thus making difficult the conduction and interpretation of kinetic experiments.[41, 42] Another substrate that we tested in preliminary experiments with copper(II) salts was the dopamine metabolite 3,4-dihydroxyphenylacetic acid, but also in this case it was impossible to trap the *o*-quinone, since it is also unstable and rapidly undergoes polymerization, as previously observed.[43]

We then chose to investigate the oxidation of two model catechol compounds: 3,5-di-*tert*-butyl catechol ($DTBCH_2$) and 4-methylcatechol (4-MC). Compared with dopamine ($E°_{pH7}$ = 0.53 V[41] – see also Table S1 for redox potential conversion), these catechols have slightly lower redox potentials, due to the electron donating substituents ($E°_{pH7}$ = 0.39 V[44] and $E°_{pH7}$ = 0.46 V[44] for $DTBCH_2$ and 4-MC, respectively). The first one has the advantage of giving a stable quinone (DTBQ) that can be observed without formation of further products. On the other hand, this catechol is not soluble in aqueous solution and requires the presence of a cosolvent like methanol. For this reason, the oxidation of water-soluble 4-MC was also studied. With this substrate, the rate of oxidation is slower compared to that of $DTBCH_2$ (see below) and the formation of quinone is followed by reaction with excess substrate to give conjugation products. To overcome these limitations, the oxidation of 4-MC was also studied in the presence of 3-methyl-2-benzothiazolinone hydrazone (MBTH), which forms a stable adduct with quinones characterized by a high extinction coefficient. This study allows also to compare data from related experiments performed using copper complexes with different peptides relevant to other neurodegenerative diseases.[45, 46]

Unlike the reaction with catechols, free copper is unable to oxidize phenolic substrates. The presence of MBTH allows to promote phenol hydroxylation due to its dual role: as a reducing agent for copper(II), and as a trapping agent for the quinone formed upon phenol hydroxylation.[46-48]

Catalytic oxidation of $DTBCH_2$

The oxidation of $DTBCH_2$ promoted by both free copper and copper-αSyn15 complex follows a biphasic behavior, as shown in Figure 1 by the black and grey continuous traces, respectively.

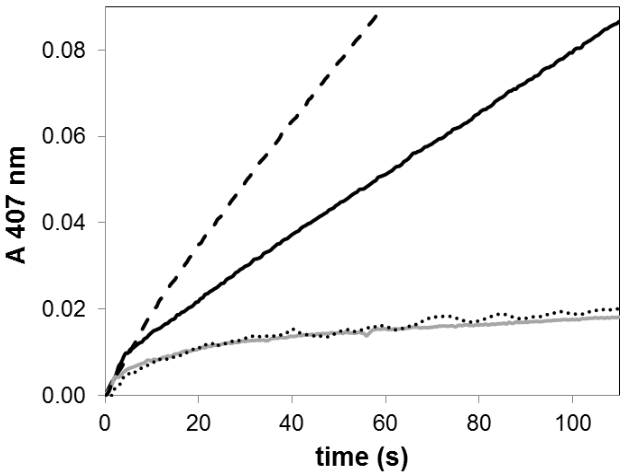

Figure 1 – Kinetic traces of absorbance at 407 nm *vs.* time for the oxidation of $DTBCH_2$ (4 mM) in a mixture of 80:20 = methanol:HEPES buffer (50 mM), pH 7.4, at 25 °C in the presence of free copper(II) (25 μM) (black continuous trace), and copper(II) (25 μM) and αSyn15 (50 μM) (gray continuous trace). The same experiment has been carried out in the same conditions with the solvent mixture saturated with pure oxygen with both free copper(II) (black dashed line) and copper-αSyn15 1:2 complex (black dotted line).

With free Cu^{2+}, the initial fast step is concluded within the first 5 s of reaction (Figure 1, black continuous trace) and the rate change becomes more evident at low substrate concentration (Figure S1). On the other hand, with both complexes [Cu^{2+}-αSyn15] (Figure 1, gray continuous trace) and [Cu^{2+}-αSyn6] (Figure S2), this step lasts about 20-30 s. In all cases, the maximum absorption of the band developed within the first step is located at approximately 396 nm, whereas the maximum shifts to 407 nm, corresponding to DTBQ formation, during catalytic turnover (Figure S3). The first intermediate with absorption at 396 nm is probably 3,5-di-*tert*-butyl-semiquinone (DTBsQ), that is formed by reaction of $DTBCH_2$ with Cu^{2+} and then dismutates to $DTBCH_2$ and DTBQ (reaction (4) below and Scheme S1).

The second part of the kinetic trace is linear and represents the catalytic cycle of $DTBCH_2$ oxidation, which is controlled by the rate limiting, second step of the reaction. The rate of this second step is dependent on copper concentration (Figure S4) and substrate concentration (see below), both in the presence of free copper or copper-αSyn peptide complex.

In order to gain more information regarding the catalytic cycle, experiments under O_2 saturating conditions were performed by varying the substrate concentration and using either free Cu^{2+} or [Cu^{2+}-αSyn15] complex as catalyst. With free copper, the rate of the catalytic process increases upon increasing O_2 concentration (Figure 1, black dashed line), whereas with [Cu^{2+}-αSyn15] the rate remains unchanged (Figure 1, black dotted line).

We can therefore propose a different mechanism when the reaction is promoted by free copper or [Cu^{2+}-αSyn15]. In both cases, the reaction depends on the concentration of copper and substrate, but with free copper also oxygen is involved in the rate determining step. In the latter case, then the mechanism involves the following reactions:

$$Cu^{2+} + DTBCH_2 \rightarrow Cu^{+} + DTBsQ \qquad (1)$$
$$Cu^{+} + O_2 \rightleftarrows Cu/O_2 \qquad (2)$$
$$Cu/O_2 + DTBCH_2 \rightarrow Cu^{2+} + DTBsQ \qquad (3)$$
$$2\,DTBsQ \rightarrow DTBCH_2 + DTBQ \qquad (4)$$

As explained above, the first step of reaction (1) is fast and stoichiometric with respect of copper concentration and gives rise to the formation of one molecule of DTBsQ, which is characterized by the absorption band at 396 nm. Reaction (2) is an equilibrium shifted to the left, because an increase in oxygen concentration gives rise to an increase of the overall reaction rate. The nature of the reactive Cu/O_2 species is unclear. Unlike catechol oxidase, or preorganized dinuclear mimetic complexes, where dioxygen binds to a pair of Cu^{+} ions, in this case a mononuclear adduct likely forms. Moreover, the reaction between copper(I) and dioxygen may also form diffusible ROS, such as superoxide, that rapidly evolves to H_2O_2 (see equations 10-11 below). In the indication of Cu/O_2 species we therefore include both copper-centred reactive species and highly reactive ROS. The third step is then associated with the formation of a second DTBsQ radical. Since reaction (4) is the fast coupling of two molecules of DTBsQ radicals to form $DTBCH_2$ and DTBQ, reaction (3) is the slow step of the catalytic cycle and (2) is a pre-equilibrium.

The reactivity observed in the presence of αSyn peptide could be due to some residual free copper, because the whole mechanism remains similar. However, the formation of a less reactive copper-αSyn peptide complex is suggested by relevant differences in the relative rates of individual steps of the mechanism proposed. In particular, the first stoichiometric reaction is slower compared to the reaction of free Cu^{2+}, as shown by the fact that it lasts until approximately 30 s. This behavior is due to the coordination of αSyn15 to Cu^{2+}, that may hinder the interaction with the substrate, or change the Cu^{2+}/Cu^{+} redox potential by stabilizing the Cu^{2+} state. Moreover, equilibrium (2) is shifted to the right because an increase of the oxygen concentration does not correspond to an increase of the overall rate. As before, reaction (3) is the slow step that depends on substrate concentration.

The catalytic rates are therefore referred to the rate determining step, which involves reaction (3) and pre-equilibrium (2). The kinetic analysis of the catalytic reactions was made using the absorbance changes in the linear portions of the absorption curves, which were taken in the interval of 5-20 s for free Cu^{2+}, and 20-40 s for [Cu^{2+}-αSyn15], respectively.

The reaction rate dependence on $DTBCH_2$ concentration shows a saturating behavior for both free copper and [Cu^{2+}-αSyn15], and could be fitted with Michaelis-Menten equation (Figure 2). In the case of Cu^{2+}, the kinetic parameters k_{cat} = (0.030 ± 0.001) s^{-1} and K_m = (0.8 ± 0.1) mM were obtained (Figure 2, black line). As αSyn15 decreases the $DTBCH_2$ oxidation rate in a concentration dependence fashion (see below), the data for [Cu^{2+}-αSyn15] shown in Figure 2 refer to the catalytic reaction studied with a ratio of Cu^{2+}:αSyn15 = 1:2, for which the following kinetic parameters were obtained k_{cat} = (0.009 ± 0.001) s^{-1} and K_m = (1.8 ± 0.2) mM (Figure 2, gray line).

It is interesting that increasing the amount of either αSyn15 or αSyn6 peptides (from 0 to 4 equivalents compared to copper concentration) induces a decrease of $DTBCH_2$ oxidation rate (Figure 3). This experiment shows that the two αSyn peptides have a very similar effect on the reaction rate, which means that their coordination to copper and the effect on the reactivity is the same, independently of the length of the chain. This

confirms that αSyn6 fragment is the shortest peptide that guarantees the copper coordination in both redox states.[31]
Coordination of αSyn peptides to Cu^{2+} significantly decreases k_{cat}, indicating reduced efficiency in the oxidation reaction. This behavior in the presence of the peptide can be explained by the following hypothesis: the equilibrium (2) is shifted to the left or the effect is primarily due to a decrease of the oxidizing capability of Cu/O_2 species. Moreover, K_m increases, indicating that also the affinity of catechol for copper is diminished by the presence of the peptide, likely because of its steric hindrance that makes the substrate coordination more difficult.

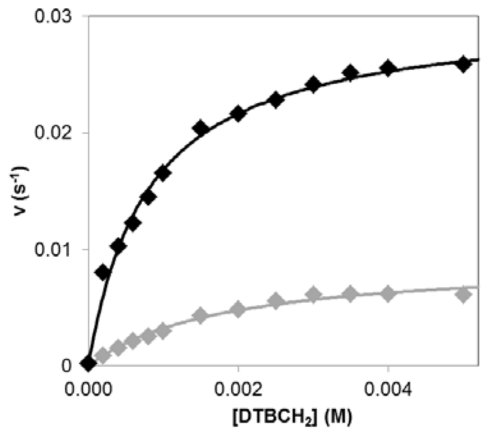

Figure 2 – Dependence of the reaction rates of DTBQ formation on the concentration of $DTBCH_2$. The reactions were performed in 80:20 = methanol:HEPES buffer (50 mM) pH 7.4, at 25 °C, in the presence of free copper(II) (black), and copper(II) (25 μM) and αSyn15 (50 μM) (gray). Solid lines correspond to fitting of experimental data with Michaelis-Menten equation.

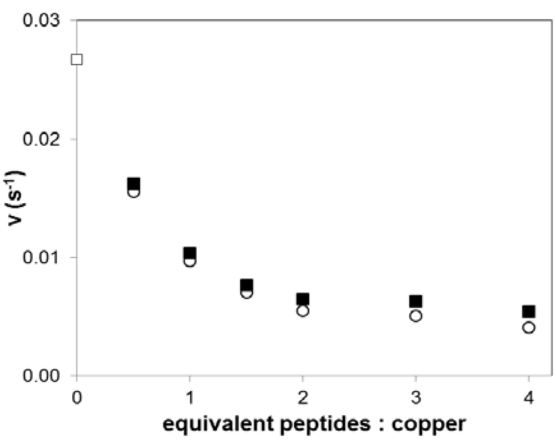

Figure 3 – Dependence of the reaction rates of DTBQ formation on the ratio between αSyn peptides and Cu^{2+} concentration. The reactions were performed in a solvent mixture of 80:20 methanol:HEPES buffer (50 mM) pH 7.4, at 25 °C, in the presence of $DTBCH_2$ (3 mM), copper(II) (25 μM) and αSyn6 (open circles) and αSyn15 (black squares) in the range of 0 to 100 μM concentration.

Catalytic oxidation of 4-MC

As explained before, the oxidation of 4-MC can be conveniently studied because this substrate is completely soluble in aqueous medium. However, the slow oxidation rate observed does not allow to perform a complete kinetic analysis, in particular with regard to the rate dependence on substrate concentration. Nevertheless, also in this case the biphasic kinetic traces of the reactions, obtained by monitoring the quinone band, show the progressive inhibitory effect exerted by the αSyn15 peptide on Cu^{2+} reactivity (Figure 4).

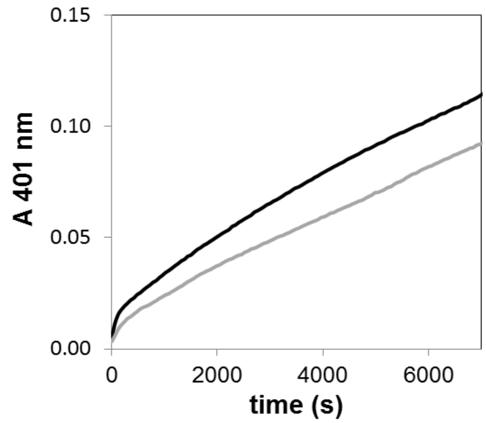

Figure 4 – Kinetic traces of absorbance at 401 nm *vs.* time for the oxidation of 4-MC (3 mM) in HEPES buffer (50 mM) at pH 7.4 and 25 °C in the presence of free Cu^{2+} (25 μM) (black trace), and Cu^{2+} (25 μM) and αSyn15 (50 μM) (gray trace).

In order to compare the reactivity of 4-MC and $DTBCH_2$ we have also performed the oxidation experiment of 4-MC in the mixture of 80:20 = methanol:HEPES buffer (50 mM). The kinetic profiles in Figure S5 show that, also in these conditions, αSyn15 peptide diminishes the reactivity of copper(II). However, the effect is more pronounced compared to aqueous solution, suggesting that solvent plays also an important role. In this case, methanol, that is less polar than water, may stabilize copper(I) redox state in the presence of αSyn peptide, making more difficult dioxygen coordination and further production of reactive species.
The reactivity observed with these catecholic substrates reflects also the redox potential relative to the reduction of the catechol to semiquinone. In particular, $DTBCH_2$ can be oxidised more easily compared to 4-MC due to the lower reduction potential (Table S1). The comparison of the redox potential may also explain the negligible oxidation of dopamine, as previously observed by Wang *et al.*.[26] Even if the technique used was the shift of DPV signal of dopamine in the presence of Cu-αSyn complex, they also observe that Cu-αSyn complex cannot directly oxidize dopamine.

Catalytic oxidation of phenol in the presence of MBTH

Free copper(II) promotes a slow oxidation of phenol in the presence of MBTH, with the formation of a MBTH-quinone adduct absorbing at 500 nm. The presence of increasing amounts of αSyn15 (Figure 5) or αSyn6 (Figure S6) progressively reduces the phenol oxidation rate.

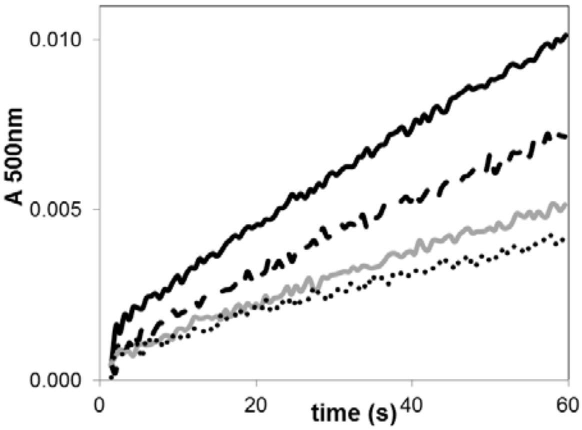

Figure 5 – Kinetic traces at 500 nm in the initial phase of reaction for the formation of the MBTH-quinone adduct by oxidation of phenol (2 mM) in the presence of Cu^{2+} (5 μM) and MBTH (2 mM) (black continuous trace) and variable amounts of αSyn15 (0.2 equiv. - black dashed trace; 0.7 equiv. – gray continuous trace; 1.5 equiv. - black dotted trace), in HEPES buffer (50 mM) at pH 7.0.

The reaction rate depends on phenol and oxygen concentrations. In fact, under saturating oxygen conditions the rate of the free Cu^{2+}-promoted oxidation of phenol increases (Figure S7). A similar effect was also observed in the reaction promoted by both [Cu^{2+}-αSyn15] and [Cu^{2+}-αSyn6] complexes.

The copper-mediated phenol oxidation is a multi-step reaction in which Cu^{2+} is rapidly reduced by MBTH (5), and Cu^{+} reacts with molecular oxygen in a pre-equilibrium binding step, giving rise to an active species capable of oxidizing the phenol to quinone.

$$Cu^{2+} + MBTH \rightarrow Cu^{+} + MBTH^{\bullet +} \quad (5)$$
$$Cu^{+} + O_2 + phenol \rightarrow \rightarrow Cu^{2+} + H_2O + quinone \quad (6)$$

The overall rate is therefore regulated by step (6) that depends on both oxygen and phenol concentration. The rate plots are hyperbolic for the reaction promoted by either free Cu^{2+}, [Cu^{2+}-αSyn15] or [Cu^{2+}-αSyn6] complexes (Figure 6). Table 1 shows that k_{cat}, referred to reaction (6), decreases in the presence of αSyn peptides, whereas the K_m values are approximately unchanged. In this case, the coordination of a less hindered substrate compared to $DTBCH_2$ is not affected by the presence of the peptide. The effect on k_{cat} is similar to the case of reaction with $DTBCH_2$ and can be explained by the shift to the left of the equilibrium involving the dioxygen coordination or by the decrease of the oxidizing capability of Cu/O_2 species.

Table 1 – Kinetic parameters for oxidation of phenol, at pH 7.0, catalyzed by Cu^{2+}, Cu^{2+}-αSyn6 and Cu^{2+}-αSyn15 complexes, in the presence of MBTH, in HEPES buffer (50 mM) at pH 7.0 at 25 °C.

Catalyst	Cu^{2+}	[Cu^{2+}-αSyn6]	[Cu^{2+}-αSyn15]
K_m (mM)	1.3 ± 0.2	1.4 ± 0.4	1.2 ± 0.5
k_{cat} (s^{-1})	$(1.64\pm0.12)\times10^{-3}$	$(0.99\pm0.12)\times10^{-3}$	$(0.72\pm0.12)\times10^{-3}$

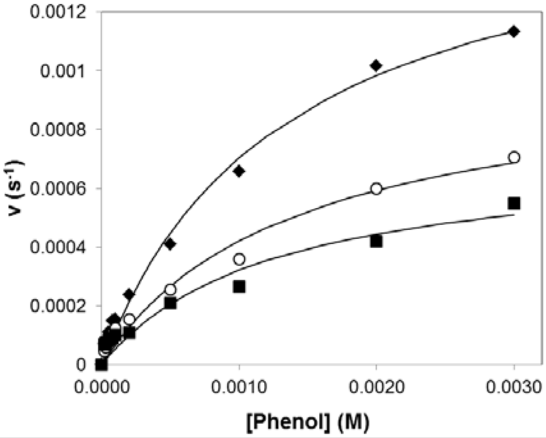

Figure 6 – Dependence of the reaction rates of MBTH-quinone formation on phenol concentration. The reactions were studied in HEPES buffer (50 mM) pH 7.0 at 25°C in the presence of free copper(II) (black diamonds), [Cu^{2+}-αSyn6] complex (open circles) or [Cu^{2+}-αSyn15] complex (black squares) at 5 μM concentration. Solid lines correspond to fit of experimental data with Michaelis-Menten equation.

Catalytic oxidation of 4-MC in the presence of MBTH

When the oxidation of 4-MC was studied in the presence of MBTH, a different behavior is observed if the catalyst is free copper or a copper-αSyn peptide complex. In the first case, the kinetic trace at 500 nm is linear, whereas in the presence of Cu^{2+}-αSyn peptides, the kinetic traces display a biphasic behavior in which the fast reaction is completed within the first ten seconds and is followed by a slower catalytic turnover compared to free Cu^{2+}. This behavior becomes more evident in the presence of excess of αSyn15 peptide (Figure 7). The same effect was observed in the presence of αSyn6 peptide (Figure S8).

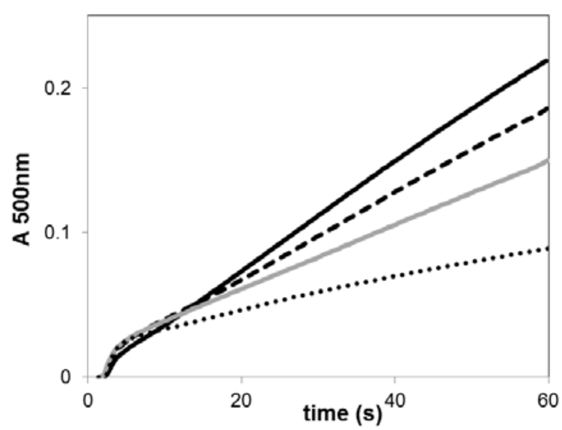

Figure 7 – Kinetic traces at 500 nm in the initial phase of oxidation of 4-MC (2 mM), with formation of MBTH-quinone adduct, in the presence of Cu^{2+} (25 μM) (black continuous trace), variable amounts of αSyn15 (0.7 equiv. - black dashed trace; 1.5 equiv. – gray continuous trace; 3.0 equiv. – black dotted trace), and MBTH (2 mM), in HEPES buffer (50 mM) at pH 7.0.

As in the Cu-mediated oxidation of phenol, the turnover rate, both in the absence and presence of αSyn peptide, increases upon replacing air with pure oxygen, indicating that the slow step of the reaction involves the formation of a Cu/O_2 intermediate. On the other hand, the first step observed in the presence of copper-αSyn complex is independent on oxygen concentration and it is related to the stoichiometric reaction with Cu^{2+} (Figure S9). Moreover, the effect of catalyst concentration is an important issue to address especially in the case of biphasic behavior, as observed in the oxidation reaction of 4-MC promoted by copper-αSyn peptide complexes. Experiments at different [Cu^{2+}-αSyn6] concentrations show that the complex concentration influences both the first rapid step and the following slow turnover (Figure 8).

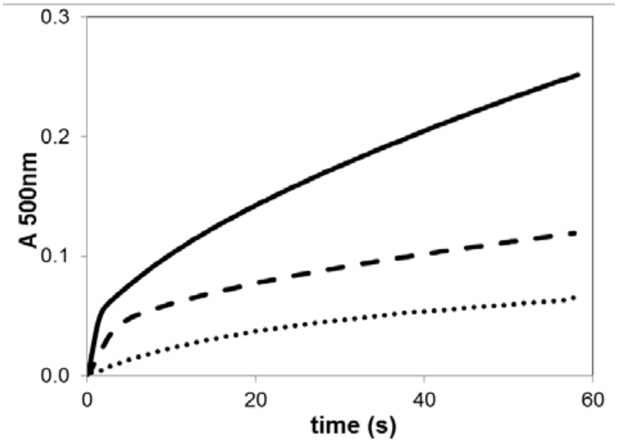

Figure 8 – Kinetic traces at 500 nm in the initial phase of oxidation of 4-MC (2 mM), with formation of MBTH-quinone adduct, in the presence of variable amounts of Cu^{2+} and αSyn6 (5 μM – dotted trace; 25 μM – dashed trace; 50 μM – continuous trace), and MBTH (2 mM), in HEPES buffer (50 mM) at pH 7.0.

The overall process is therefore controlled by the following reactions:

$$Cu^{2+} + 4\text{-MC} + MBTH \rightarrow Cu^{+} + Q\text{-}MBTH \quad (7)$$
$$Cu^{+} + O_2 + 2\,(4\text{-MC}) \rightarrow \rightarrow Cu^{2+} + 2\,H_2O + 2\text{ quinone} \quad (8)$$

The copper-αSyn peptide complex has a dual role in this reactivity: besides promoting the stoichiometric reaction (7), it decreases the turnover rate, probably lowering the Cu^+ affinity for O_2 in the formation of the $Cu\text{-}O_2$ intermediate.
The turnover rate dependence on substrate concentration shows again that the presence of αSyn peptides diminishes the catecholase activity of free Cu^{2+} in solution, even if the rate plot does not follow a Michaelis-Menten behavior, for both free copper and Cu^{2+}-peptide complexes (Figure 9).

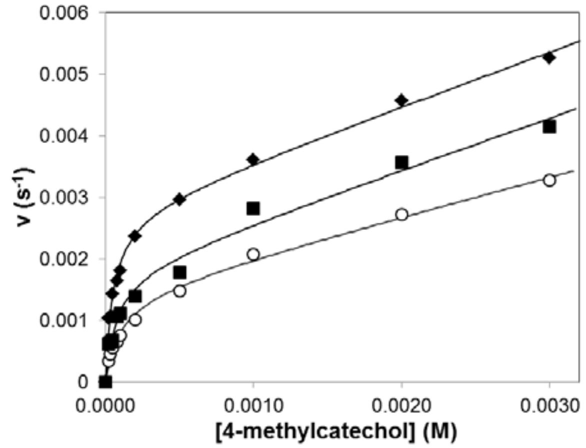

Figure 9 – Dependence of the reaction rates of MBTH-4-methylquinone formation on the concentration of 4-MC. The reactions were performed in HEPES buffer (50 mM) pH 7.0 at 25 °C in the presence of free copper(II) (black diamonds), [Cu^{2+}-αSyn6] (open circles) and [Cu^{2+}-αSyn15] (black squares) at 25 μM concentration. Solid lines correspond to fit of experimental data with trendline.

This behavior is probably due to the multiple role of MBTH in this reaction. MBTH traps the quinone formed by the reaction but it also acts as a co-substrate contributing in the reduction of copper(II) in reaction (7). Oxidised MBTH displays an absorption at 440 nm which contributes with a shoulder to the absorption at 500 nm. This effect is more evident at low 4-MC concentration, making the reaction rate in the 20-500 μM range underestimated. A similar reactivity was observed also for [Cu^{2+}-Aβ28] complex,[45] where the first step is faster in the presence of the peptide and is followed by a slower turnover.

Identification and characterization of oxidized peptide by HPLC-ESI/MS

The catalytic cycles discussed above involve the formation of a Cu^+ intermediate that reacts with oxygen to generate a Cu/O_2 species capable of oxidizing the substrate. However, unlike catechol oxidase or tyrosinase, both free copper and copper-αSyn complexes are unable to stabilize a dicopper-peroxo species. Thus, it is not surprising that free copper and copper-αSyn complexes are less efficient catalysts than genuine dicopper(II) model complexes that mimic the active site of these enzymes.[38, 39] On the other hand, this behavior has the important consequence that formation of copper(I) species can promote Fenton reactions resulting in the production of harmful ROS. In fact, according to Eqs. (9)-(11), Cu^+ can catalyze the reduction of dioxygen to ROS, i.e. H_2O_2 and $OH^{\bullet}$, that give rise to protein damage through oxidation of specific amino acid residues.

$$Cu^{+} + O_2 \rightarrow Cu^{2+} + O_2^{-} \quad (9)$$
$$2\,O_2^{-} + 2H^{+} \rightarrow O_2 + H_2O_2 \quad (10)$$
$$H_2O_2 + Cu^{+} \rightarrow OH^{-} + OH^{\bullet} + Cu^{2+} \quad (11)$$

One important target of this oxidation is αSyn itself, since it has been proposed that sulfoxidation of methionine can enhance protein aggregation. A previous NMR study shows that copper(I)-αSyn complex can oxidize the N-terminal Met-1.[31] Here, we investigate the possible competition between catechol

oxidation and oxidative modification of αSyn peptide bound to copper, a situation that partially reproduces the cellular environment in which catechols (dopamine) and αSyn protein are present at high concentration.
In these experiments, solutions of copper and αSyn15 peptide were incubated in the presence of the substrate, $DTBCH_2$ or 4-MC, in the same conditions as in the catalytic oxidations, but the mixture was then subjected to LC-MS analysis to determine the site and extent of protein modifications.
In general, LC analysis of the reaction mixtures showed the presence of three main peaks in different proportions. These correspond to the native peptide (MDVFMKGLSKAKEGV), with a retention time (t_R) of 36 min, an inseparable mixture of the two peptides containing a single oxidation on one of the two methionines (M*DVFMKGLSKAKEGV and MDVFM*KGLSKAKEGV), with a t_R of 34 min, and a third peak identified as the peptide undergoing oxidation at both methionine residues (M*DVFM*KGLSKAKEGV), with a t_R of 31 min (Figure 10, top). MS/MS analysis of the peptide modified with two oxygen atom insertion excludes the formation of sulfone after double oxidation of a single methionine.

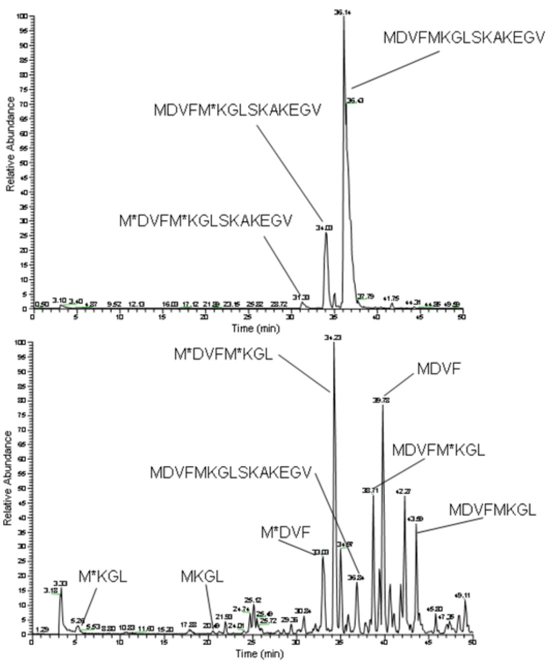

Figure 10 – HPLC-MS elution profiles of αSyn15 incubated in the presence of copper(II) and 4-MC before (top) and after (bottom) proteolytic digestion with chymotrypsin. The assignment of the peaks is shown.

As shown in Table 2, in the reaction involving $DTBCH_2$, αSyn15 peptide is only slightly modified with the formation of small percentage of a single oxidation on one of the two methionines.

Table 2 – Oxidation of methionine residues as a function of time and $DTBCH_2$ concentration detected by HPLC-MS analysis, in the presence of 25 μM copper(II) nitrate and 50 μM αSyn15 in HEPES buffer (50 mM) pH 7.4 at 25 °C.

Time (h)	[$DTBCH_2$] (mM)	% single oxidation	% double oxidation
2	3.0	2	0.1
9	3.0	6	0.5
2	0.8	1	0.0
72	0.8	9	0.0

On the other hand, in the presence of 4-MC the percentage of formation of single oxidized and double oxidized peptide is much higher, as shown in Table 3, and strongly depends on incubation time.

Table 3 – Oxidation of methionine residues as a function of time and 4-MC concentration detected by HPLC-MS analysis, in the presence of 25 μM copper(II) nitrate and 50 μM αSyn15 in Hepes buffer (50 mM) pH 7.4 at 25 °C.

Time (h)	[4-MC] (mM)	% single oxidation	% double oxidation
2	0.8	8	0.3
72	0.8	36	41
2	3.0	18	10
7	3.0	44	22
72	3.0	4	73

The difference in reactivity between the two substrates may be related to the stability of the semiquinone species. DTBsQ is relatively stable and sterically hindered, and is accumulated during the reaction, as observed in the kinetic analysis, without the capability to promote secondary reactions. On the contrary, 4-methylsemiquinone (4-MC•) is not stable and once generated undergoes rapid reactions to give a dimeric coupling product (Eq. 12) or radical reaction on the peptide methionine sulfur (Eq. 13), which is then easily oxidized to sulfoxide (Eq. 14).

$$4\text{-MC}^\bullet + 4\text{-MC}^\bullet \rightarrow \text{dimer} \quad (12)$$
$$4\text{-MC}^\bullet + \text{Met(SH)} \rightarrow 4\text{-MC} + \text{Met(SH)}^{+\bullet} \quad (13)$$
$$\text{Met(SH)}^{+\bullet} + \text{Met(SH)}^{+\bullet} + H_2O \rightarrow 3H^+ + \text{Met(S=O)} + \text{Met(SH)} \quad (14)$$

It is also important to understand if this copper-mediated oxidation is limited to αSyn directly bound to the metal (*intra*-molecular mechanism) or if the oxidation is extended to non-coordinated peptide (*inter*-molecular mechanism). For this reason, we performed different oxidation experiments with variable copper/αSyn15 ratios, and analyzed the peptides by LC-MS after the same reaction time (2 h).
If an *inter*–molecular mechanism were operative, the amount of oxidized peptide should increase by increasing the peptide concentration, independently of copper concentration, whereas according to an *intra*-molecular mechanism the amount of oxidized peptide should depend on copper concentration. As shown by the data in Table 4, the amount of oxidized peptide

depends on peptide concentration and this effect is more evident comparing the absolute concentration of oxidized peptide. This behavior indicates that also unbound αSyn15 peptide can be oxidized by copper with an *inter*-molecular mechanism.

Table 4 – Oxidation of methionine residues as a function of αSyn15 peptide concentration detected by HPLC-MS analysis after 2 h of reaction time, in the presence of 25 μM copper(II) nitrate in HEPES buffer (50 mM) pH 7.4 at 25 °C.

[αSyn15] (μM)	% single oxidation	[αSyn15 oxidised] (μM)	% double oxidation
50	16	8	0.5
100	13	13	0.3
150	9	14	0.2
200	9	18	0.2

To establish which methionine residue between Met1 and Met5 is more sensitive to oxidation, we performed a proteolytic digestion of αSyn15 with chymotrypsin. This enzyme selectively cleaves peptide chains after Tyr, Phe, Trp, and Leu residues. As expected, the chromatograms show several peaks, corresponding to the fragments obtained upon αSyn15 cuts at Phe and Leu residues (Figure 10 bottom). In particular, MS/MS data allowed the identification of the following peptides containing Met residues in their native (M) or oxidized (M*) form: MKGL, M*KGL, MDVF, M*DVF, MDVFMKGL, M*DVFM*KGL and MDVFM*KGL. However, this analysis does not permit to identify any particular preference towards the oxidation of Met1 or Met5, and both residues are equally oxidized. The “random” oxidation is in agreement with the reaction mechanism proposed in the kinetic analysis, where the copper-mediated mechanism is able to oxidize an external peptide chain through an *inter*-molecular mechanism, that is intrinsically non regiospecific.

In previous literature data, Zhou *et al.*,[49] indicate that Met5 is oxidized more easily, whereas recent studies by Miotto *et al.*,[31] report that oxidation of Met1 is faster than oxidation of Met5. This controversy supports the conclusion that oxidation of both methionines is possible.

SOD activity

The SOD-like activity of [Cu^{2+}-αSyn6] and [Cu^{2+}-αSyn15] complexes was compared to activity of free Cu^{2+} in solution. The activity was evaluated through the direct assay in which O_2^- is directly generated by dissolution of KO_2 salt and detected by the reaction with nitro blue tetrazolium (NBT), which forms methyl formazane (MF^+), characterized by an intense absorption band at 560 nm.[50] MF^+ formation is diminished by the presence of micromolar concentration of Cu^{2+} in solution (Figure 11). However, the same behavior is displayed by both [Cu^{2+}-αSyn6] and [Cu^{2+}-αSyn15], indicating that binding of αSyn peptides to Cu^{2+} does not alter the intrinsic superoxide dismutase reactivity of copper ion. A similar result was obtained with [Cu^{2+}-Aβ16] and [Cu^{2+}–Aβ28] complexes.[45]

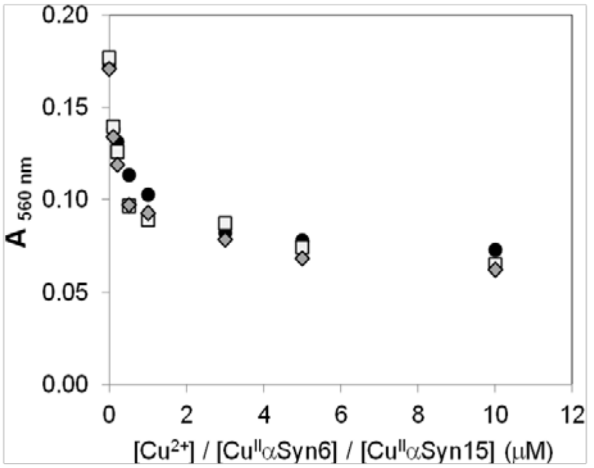

Figure 11 – Plots of UV-Vis absorbance at 560 nm for the NBT reduction to MF^+ by O_2^- in the presence of Cu^{2+} (open squares), [Cu^{2+}-αSyn15] (black circles), and [Cu^{2+}-αSyn6] (gray diamonds). Spectra were taken at 25 °C, in 50 mM aqueous phosphate buffer, pH 7.4.

Experimental

General methods

The N-terminal αSyn15 and αSyn6 peptides, with sequence ^{1}MDVFMKGLSKAKEGV^{15} and ^{1}MDVFMK^{6}, respectively, were synthesized in solid phase using Fmoc chemistry. Rink-amide resin was used as the solid support so that the resulting peptides will be amidated at the C-terminus. After removal of the peptides from the resin and deprotection, the crude products were purified by RP HPLC on a Phenomenex Jupiter 4u Proteo column (4 μm), 250×10 mm, using a Jasco PU-1580 instrument with diode array detection (Jasco MD-1510), using a semi-linear gradient of 0.1% TFA in water to 0.1% TFA in CH_3CN over 40 min. The purified peptides were lyophilized and stored at -20 °C until use. The identity of the peptide was confirmed by Electrospray ionization mass spectrometry (Thermo-Finnigan). Kinetic experiments were performed on an Agilent 8453 spectrophotometer and monitored between 190 and 1100 nm using an optical cell with magnetic stirring and 1 cm path length. The reactants were mixed under magnetic stirring in a thermostated cell at 25.0±0.5 °C. All chemicals were reagent grade and purchased from Sigma-Aldrich.

Catalytic oxidation of $DTBCH_2$ in the presence of copper(II), [Cu^{2+}-αSyn6] and [Cu^{2+}-αSyn15] complexes

The catalytic oxidation of $DTBCH_2$ by Cu^{2+} and O_2 was studied at room temperature in a mixed solvent of 80/20 (v/v) methanol-aqueous 50 mM 4-(2-hydroxyethyl)-1-piperazine ethanesulfonic acid (HEPES) buffer at pH 7.4, saturated with atmospheric oxygen. The reactions were followed through the development of the 3,5-di-*tert*-butylquinone (DTBQ) band at 407 nm for 120 s reaction time. Within this reaction time also the DTBsQ formation (with a broad band centered at 396 nm) slightly contributes to the absorbance changes; however, at 407 nm the spectral changes are mostly dominated by the DTBQ band and we therefore considered the contribution of DTBsQ negligible in the analysis of the rate data. An ε value of 1500 $M^{-1}cm^{-1}$ for the oxidation product was determined by acquiring absorption spectra of solutions of known concentration of

commercial DTBQ. The rate dependence on [$DTBCH_2$] was determined by maintaining the concentration of copper(II) nitrate or copper-αSyn15 (1:2) 25 μM and varying the substrate concentration from 0.02 to 4.0 mM. All measurements were performed in duplicate.
The kinetic traces showed a biphasic behavior, as reported in the Results and Discussion paragraph. The conversion from ΔA/s to s^{-1} units was made using the quinone extinction coefficient and the copper concentration. Blank experiments on the oxidation of $DTBCH_2$ under the same conditions but in the absence of Cu^{2+} showed that autoxidation of the substrate was negligible.
The effect of αSyn peptides (both αSyn6 or αSyn15) on the copper-catalyzed $DTBCH_2$ oxidation was analyzed by adding the peptide in variable stoichiometry, from 0 to 4 equivalents with respect to Cu^{2+}, to the reaction solution containing $DTBCH_2$ (3 mM), followed by copper(II) nitrate (25 μM) as the last reagent. To assess the effect of oxygen concentration on the reaction rate, the $DTBCH_2$ (4 mM) oxidation experiments were also performed in oxygen saturating conditions, which were obtained by bubbling pure dioxygen (1 atm) into the methanol:buffer solution.

Catalytic oxidation of 4-methyl-catechol in the presence of copper(II) and [Cu^{2+}-αSyn15] complex

The catalytic oxidation of 4-MC by Cu^{2+} and O_2 was studied at room temperature in 50 mM HEPES buffer at pH 7.4, saturated with atmospheric oxygen. The reactions were followed through the development of the 4-methyl-quinone band at 401 nm for 7200 s reaction time. An ε value of 1550 $M^{-1}cm^{-1}$ for the oxidation product was determined by employing tyrosinase as the catalyst in the same conditions of activity measurements. The slow rate observed with this catechol does not allow to determine the rate dependence on the concentration of the substrate. The concentrations of copper(II) nitrate and substrate were kept constant at 25 μM and 3 mM, respectively. All measurements were performed in duplicate. Blank experiments on the oxidation of 4-MC under the same conditions but in the absence of Cu^{2+} showed that a slow autoxidation of the substrate is present. The kinetic trace showed a biphasic behavior, as reported in the Results and Discussion paragraph. The different kinetic behavior in the presence of copper-peptide complexes was evaluated by comparing the kinetic traces at 401 nm. The αSyn15 peptide was added, in 2:1 ratio with respect to Cu^{2+}, to the solution of 4-MC (3 mM), followed by copper(II) nitrate (25 μM) as the last reagent.

Catalytic oxidation of phenol and catechol in the presence of 3-methyl-2-benzothiazolinone hydrazone (MBTH), copper(II), [Cu^{2+}-αSyn6] and [Cu^{2+}-αSyn15] complexes

Effect of the substrate concentration. Phenol hydroxylation and catechol oxidation experiments with [Cu^{2+}-αSyn6] or [Cu^{2+}-αSyn15] were carried out by reacting equimolar concentrations of phenol, or 4-MC, and MBTH (typically from 0.02 to 3.0 mM) in 50 mM HEPES buffer at pH 7.0 in the presence of the Cu-αSyn complex (typically from 5 to 25 μM). The phenol hydroxylation and 4-methylcatechol oxidation experiments were repeated using copper(II) nitrate at the same concentration as [Cu^{2+}-αSyn]. The formation of the red adduct between the quinone product and MBTH was monitored at 500 nm (ε = 32500 $M^{-1}cm^{-1}$).[46]
The turnover rates (s^{-1}) were obtained by dividing the initial absorbance changes (typically 5-20 s) with time (ΔAbs/s) for the catalyst concentration, the optical path length (1 cm) and the extinction coefficient of the product. Blank experiments of oxidation of phenol and 4-methylcatechol under the same conditions, but in the absence of free copper or [Cu^{2+}-αSyn] showed that autoxidation of the substrate was negligible.
Effect of the copper(II)/peptide ratio. Phenol hydroxylation and 4-MC oxidation experiments were performed in 50 mM HEPES buffer at pH 7.0 equilibrated with atmospheric oxygen and containing 2 mM phenol, or 4-MC, and 2 mM MBTH. The reactions started upon adding the peptide (in variable amount) and copper(II) nitrate (5 – 25 μM) to the solution. The kinetic traces of the reactions, obtained by monitoring the band of the red MBTH-quinone adduct at 500 nm, showed the progressive inhibitory effect exerted by αSyn6 and αSyn15 peptides.
Effect of oxygen concentration. Phenol hydroxylation and 4-MC oxidation experiments were also performed in oxygen saturated conditions, which were obtained by bubbling the buffer solution with pure dioxygen (1 atm). With the Cu complexes of both peptides, oxidation experiments were performed in 50 mM HEPES buffer at pH 7.0 and containing 2 mM phenol, or 4-MC, and 2 mM MBTH.
Effect of catalyst concentration. 4-MC (2 mM) oxidation experiments were performed in 50 mM HEPES buffer at pH 7.0 in the presence and variable amounts of [Cu^{2+}-αSyn6] complex (5, 25, 50 μM).

Identification and characterization of oxidized peptides by HPLC-ESI/MS

Peptide modification was analyzed performing experiments in the same conditions used for oxidation studies by HPLC-ESI/MS. When $DTBCH_2$ was used as substrate, samples were prepared in the presence of copper(II) nitrate (25 μM), αSyn15 peptide (50 μM) and $DTBCH_2$ (0.8 or 3 mM) in 80:20 (v/v) methanol:HEPES buffer (50 mM) pH 7.4. HPLC-MS analysis was performed at different reaction times: 2, 9 or 72 h. In the experiments where 4-MC was the substrate, samples were prepared in the presence of copper(II) nitrate (25 μM), αSyn15 (50 μM) and 4-MC (0.8 or 3 mM) in HEPES buffer (50 mM) pH 7.4. HPLC-MS analysis was performed at different reaction times: 2, 7 or 72 h.
In the experiments where the copper:αSyn ratio was changed, the following conditions were used: copper(II) nitrate (25 μM), αSyn15 (50, 100, 150 and 200 μM), and 4-MC (3 mM) were allowed to react in HEPES buffer (50 mM) pH 7.4. After 2 h reaction time, samples were frozen in liquid nitrogen and further analyzed by HPLC-MS.
Fragmentation of αSyn15 after the reaction of copper(II) nitrate (25 μM), the peptide (50 μM), and 4-MC (3 mM) in 50 mM HEPES buffer at pH 7.4, was performed by chimotrypsin digestion. The enzyme was prepared in acidic water (0.1 % HCl) at 1 mg/ml concentration and added in 1:50 ratio (w/w) with respect to the peptide after 2 h reaction. The digestion was performed in a thermostated bath at 37 °C for 3 h. Autoxidation of methionine in HEPES buffer at pH 7.4 was found to be negligible (below 1 %) even at 72 h reaction time.
LC–MS and LC–MS/MS data were obtained by using the LCQ ADV MAX ion-trap mass spectrometer. The system was run in automated LC–MS/MS mode and using a Surveyor HPLC system (Thermo Finnigan, San Jose, CA, USA) equipped with a Phenomenex Jupiter 4u Proteo column (4 µm, 150×2.0 mm). The elution was performed by using 0.1% HCOOH in distilled water (solvent A) and 0.1% HCOOH in acetonitrile (solvent B), with a flow rate of 0.2 ml/min; elution started with 98% solvent A for 5 min followed by a linear gradient from 98 to 55% A in 65 min for 4-MC oxidation experiments (including analysis of proteolytic fragments obtained with chymotrypsin), and with 80% solvent A for 5 min followed by a linear gradient from 80 to 50% A in 60 min for

DTBCH_2 oxidation experiments, respectively. MS/MS experiments by collision-induced dissociation (CID) were performed with an isolation width of 2 Th (*m/z*); the activation amplitude was around 35% of the ejection radiofrequency (RF) amplitude of the instrument. For the analysis of peptide fragments, Bioworks 3.1 and Xcalibur 2.0.7 SP1 software were used (Thermo Finnigan, San Jose, CA (USA)).

Superoxide dismutase activity

The assay to determine the SOD activity of free Cu^{2+} and Cu-αSyn complexes was performed as recently described by our group.[45] In this direct assay superoxide is generated by dissolution of KO_2 in DMSO in the presence of 18-crown-6 ether, and the reaction between O_2^- and NBT is followed through the development of the characteristic band at 560 nm of MF^+. In the presence of compounds promoting O_2^- disproportionation, the SOD activity is determined by the reduced intensity of the absorption band at 560 nm.

Conclusions

The reactivity of copper(II)-αSyn peptide complexes in oxidative reactions and superoxide dismutation were studied with the aim of elucidating the contribution of copper-αSyn interaction to the etiology of PD. In general, αSyn15 and αSyn6 peptides display similar behaviour in the reactivity studies performed. This trend confirms previous spectroscopic and structural studies showing that αSyn6 is the essential unit reproducing the copper coordination in both oxidation states.[13, 31] The main conclusion from these studies is that copper-αSyn complexes exhibit no significant pseudo-enzymatic activity, in particular superoxide dismutase and tyrosinase-like (phenol monoxygenase and diphenol oxidase) reactivities. This behavior is probably due to the different coordination environment of the Cu^{2+} and Cu^+ ions in the peptide, that requires a structural rearrangement in the metal coordination sphere in every reaction involving Cu^{2+}/Cu^+ cycling. The addition of an αSyn peptide diminishes the oxidative reactivity of free copper(II) in solution, by making dioxygen coordination to copper(I) more difficult or by decreasing the oxidizing capability of the resulting Cu/O_2 species.

On the other hand, redox cycling of Cu^{2+}/Cu^+ ions may cause concomitant modifications of αSyn itself through radical Fenton-like reactions. In particular, the HPLC-MS analysis of solutions of αSyn15 peptide incubated with copper and catechols shows that αSyn is susceptible to sulfoxidation at both Met1 and Met5. Using DTBC as an external substrate, the percentage of αSyn15 methionine sulfoxide is very low, indicating that an electron-rich substrate is able to protect the peptide from oxidation. In contrast, a significant amount of oxidation of both αSyn15 Met1 and Met5 is found when the less oxidizable 4-MC is used as external substrate. Most importantly, sulfoxidation also occurs on peptide not directly bound to copper, indicating that external αSyn can be oxidized by copper. This aspect has some relevance for the development of PD because oxidative modifications of αSyn were proposed to play a role in its aggregation and numerous studies focused on the structural and cellular consequences of αSyn oxidation.[51]

In particular, the sulfoxidation of methionine residues seems to inhibit amyloid fibril formation but promotes the formation of stable αSyn oligomers.[24, 49] Moreover, in the cytosol several enzymes, and in particular methionine sulfoxide reductases, are involved in the repair of methionine sulfoxidation,[23, 25] suggesting that αSyn may act as a catalytically regenerated scavenger of oxidants in physiological conditions, thus performing an important protective role prior to the development of PD. Our study suggests that copper can have an important role in the regulation of this fine mechanism in both physiological and pathological conditions.

However, recent evidence reporting the N-acetylation of αSyn in mammals suggests the coordination of copper(II) to this protein portion is lost.[22] The coordination of copper(I) has not been investigated yet, but the binding involving the side chains of Met1, Asp2, Met5 should not be abolished in the acetylated protein. In this light, the redox properties and the reactivity of the Cu^{2+}/Cu^+-N-acetyl-αSyn complexes will need to be investigated in detail.

Finally, sulfoxidation of methionine residues diminishes the coordinative property of this residue and this modification would lead to a decrease of the affinity of αSyn for copper(I). For this reason, further studies regarding the binding affinity of copper(I) to the N-terminal region of αSyn before and after sulfoxidation are required to fully elucidate this complex reactivity pattern.

Acknowledgements

This work was supported by the Italian MIUR, through the PRIN (Programmi di Ricerca di Rilevante Interesse Nazionale) project 2010M2JARJ_004. The COST CM1003 Action and CIRCMSB are also gratefully acknowledged.

Notes and references

[a] Dipartimento di Chimica, Università di Pavia, Via Taramelli 12, 27100 Pavia, Italy.

[b] Dipartimento di Biotecnologie, Chimica e Farmacia, Università di Siena, Via A. Moro 2, 53100 Siena, Italy.

Electronic Supplementary Information (ESI) available: reaction scheme of oxidation of catecholic substrates, additional information regarding redox potential of catecholic substrates, additional kinetic profiles of oxidation experiments. See DOI: 10.1039/b000000x/

1. M. Goedert, *Nat Rev Neurosci*, 2001, **2**, 492-501.
2. J. Burré, M. Sharma, T. Tsetsenis, V. Buchman, M. R. Etherton and T. C. Südhof, *Science*, 2010, **329**, 1663-1667.
3. S. Yu, K. Uéda and P. Chan, *Mol Neurobiol*, 2005, **31**, 243-254.
4. A. Sidhu, C. Wersinger and P. Vernier, *FASEB J*, 2004, **18**, 637-647.
5. H.-J. Lee, E.-J. Bae and S.-J. Lee, *Nat Rev Neurol*, 2014, **10**, 92-98.
6. H. A. Lashuel, C. R. Overk, A. Oueslati and E. Masliah, *Nat Rev Neurosci*, 2013, **14**, 38-48.
7. M. G. Spillantini, M. L. Schmidt, V. M. Lee, J. Q. Trojanowski, R. Jakes and M. Goedert, *Nature*, 1997, **388**, 839-840.
8. E. Gaggelli, H. Kozlowski, D. Valensin and G. Valensin, *Chem Rev*, 2006, **106**, 1995-2044.
9. H. Kozlowski, M. Luczkowski, M. Remelli and D. Valensin, *Coordination Chemistry Reviews*, 2012, **256**, 2129-2141.
10. A. Binolfi, L. Quintanar, C. W. Bertoncini, C. Griesinger and C. O. Fernández, *Coordination Chemistry Reviews*, 2012, **256**, 2188-2201.
11. A. Binolfi, R. M. Rasia, C. W. Bertoncini, M. Ceolin, M. Zweckstetter, C. Griesinger, T. M. Jovin and C. O. Fernández, *J Am Chem Soc*, 2006, **128**, 9893-9901.

12. R. M. Rasia, C. W. Bertoncini, D. Marsh, W. Hoyer, D. Cherny, M. Zweckstetter, C. Griesinger, T. M. Jovin and C. O. Fernández, *Proc Natl Acad Sci U S A*, 2005, **102**, 4294-4299.
13. A. Binolfi, E. E. Rodriguez, D. Valensin, N. D'Amelio, E. Ippoliti, G. Obal, R. Duran, A. Magistrato, O. Pritsch, M. Zweckstetter, G. Valensin, P. Carloni, L. Quintanar, C. Griesinger and C. O. Fernández, *Inorg Chem*, 2010, **49**, 10668-10679.
14. A. Binolfi, G. R. Lamberto, R. Duran, L. Quintanar, C. W. Bertoncini, J. M. Souza, C. Cerveñansky, M. Zweckstetter, C. Griesinger and C. O. Fernández, *J Am Chem Soc*, 2008, **130**, 11801-11812.
15. D. Valensin, F. Camponeschi, M. Luczkowski, M. C. Baratto, M. Remelli, G. Valensin and H. Kozlowski, *Metallomics*, 2011, **3**, 292-302.
16. J. C. Lee, H. B. Gray and J. R. Winkler, *J Am Chem Soc*, 2008, **130**, 6898-6899.
17. M. S. Jackson and J. C. Lee, *Inorg Chem*, 2009, **48**, 9303-9307.
18. L. Hong and J. D. Simon, *The Journal of Physical Chemistry B*, 2009, **113**, 9551-9561.
19. C. G. Dudzik, E. D. Walter and G. L. Millhauser, *Biochemistry*, 2011, **50**, 1771-1777.
20. T. Bartels, J. G. Choi and D. J. Selkoe, *Nature*, 2011, **477**, 107-110.
21. B. Fauvet, M. K. Mbefo, M.-B. Fares, C. Desobry, S. Michael, M. T. Ardah, E. Tsika, P. Coune, M. Prudent, N. Lion, D. Eliezer, D. J. Moore, B. Schneider, P. Aebischer, O. M. El-Agnaf, E. Masliah and H. A. Lashuel, *Journal of Biological Chemistry*, 2012, **287**, 15345-15364.
22. G. M. Moriarty, C. A. S. A. Minetti, D. P. Remeta and J. Baum, *Biochemistry*, 2014, **53**, 2815-2817.
23. S. Schildknecht, H. R. Gerding, C. Karreman, M. Drescher, H. A. Lashuel, T. F. Outeiro, D. A. Di Monte and M. Leist, *J Neurochem*, 2013, **125**, 491-511.
24. N. B. Cole, D. D. Murphy, J. Lebowitz, L. Di Noto, R. L. Levine and R. L. Nussbaum, *Journal of Biological Chemistry*, 2005, **280**, 9678-9690.
25. A. S. Maltsev, J. Chen, R. L. Levine and A. Bax, *Journal of the American Chemical Society*, 2013, **135**, 2943-2946.
26. C. Wang, L. Liu, L. Zhang, Y. Peng and F. Zhou, *Biochemistry*, 2010, **49**, 8134-8142.
27. P. Davies, X. Wang, C. J. Sarell, A. Drewett, F. Marken, J. H. Viles and D. R. Brown, *Biochemistry*, 2011, **50**, 37-47.
28. F. Camponeschi, D. Valensin, I. Tessari, L. Bubacco, S. Dell'Acqua, L. Casella, E. Monzani, E. Gaggelli and G. Valensin, *Inorg Chem*, 2013, **52**, 1358-1367.
29. A. Binolfi, A. A. Valiente-Gabioud, R. Duran, M. Zweckstetter, C. Griesinger and C. O. Fernandez, *J Am Chem Soc*, 2011, **133**, 194-196.
30. R. De Ricco, D. Valensin, S. Dell'Acqua, L. Casella, E. Gaggelli, G. Valensin, L. Bubacco and S. Mangani, *Inorg Chem*, 2015, **54**, 265-272.
31. M. C. Miotto, E. E. Rodriguez, A. A. Valiente-Gabioud, V. Torres-Monserrat, A. Binolfi, L. Quintanar, M. Zweckstetter, C. Griesinger and C. O. Fernández, *Inorg Chem*, 2014, **53**, 4350-4358.
32. H. R. Lucas, S. Debeer, M. S. Hong and J. C. Lee, *J Am Chem Soc*, 2010, **132**, 6636-6637.
33. G. Meloni and M. Vašák, *Free Radic Biol Med*, 2011, **50**, 1471-1479.
34. S. L. Leong, C. L. Pham, D. Galatis, M. T. Fodero-Tavoletti, K. Perez, A. F. Hill, C. L. Masters, F. E. Ali, K. J. Barnham and R. Cappai, *Free Radic Biol Med*, 2009, **46**, 1328-1337.
35. S. Ayton, P. Lei, J. A. Duce, B. X. Wong, A. Sedjahtera, P. A. Adlard, A. I. Bush and D. I. Finkelstein, *Ann Neurol*, 2013, **73**, 554-559.
36. K. M. Davies, S. Bohic, A. Carmona, R. Ortega, V. Cottam, D. J. Hare, J. P. Finberg, S. Reyes, G. M. Halliday, J. F. Mercer and K. L. Double, *Neurobiol Aging*, 2014, **35**, 858-866.
37. E. I. Solomon, D. E. Heppner, E. M. Johnston, J. W. Ginsbach, J. Cirera, M. Qayyum, M. T. Kieber-Emmons, C. H. Kjaergaard, R. G. Hadt and L. Tian, *Chemical Reviews*, 2014, **114**, 3659-3853.
38. E. A. Lewis and W. B. Tolman, *Chemical Reviews*, 2004, **104**, 1047-1076.
39. G. Battaini, A. Granata, E. Monzani, M. Gullotti and L. Casella, in *Adv. Inorg. Chem.*, 2006 vol. 58 pp. 185-233.
40. J. A. Obeso, M. C. Rodriguez-Oroz, C. G. Goetz, C. Marin, J. H. Kordower, M. Rodriguez, E. C. Hirsch, M. Farrer, A. H. Schapira and G. Halliday, *Nat Med*, 2010, **16**, 653-661.
41. A. N. Pham and T. D. Waite, *J Inorg Biochem*, 2014, **137**, 74-84.
42. E. Herlinger, R. F. Jameson and W. Linert, *Journal of the Chemical Society, Perkin Transactions 2*, 1995, 259-263.
43. R. P. Ferrari, S. Traversa, L. De Gioia, P. Fantucci, G. Suriano and E. M. Ghibaudi, *J Biol Inorg Chem*, 1999, **4**, 12-20.
44. A. Nemeikaite-Ceniene, A. Imbrasaite, E. Sergediene and N. Cenas, *Arch Biochem Biophys*, 2005, **441**, 182-190.
45. D. Ciregna, E. Monzani, G. Thiabaud, S. Pizzocaro and L. Casella, *Chem Commun (Camb)*, 2013, **49**, 4027-4029.
46. G. F. da Silva and L. J. Ming, *Angew Chem Int Ed Engl*, 2005, **44**, 5501-5504.
47. J. N. Rodríguez-López, J. Escribano and F. García-Cánovas, *Anal Biochem*, 1994, **216**, 205-212.
48. R. P. Ferrari, E. Laurenti, E. M. Ghibaudi and L. Casella, *Journal of Inorganic Biochemistry*, 1997, **68**, 61-69.
49. W. Zhou, C. Long, S. H. Reaney, D. A. Di Monte, A. L. Fink and V. N. Uversky, *Biochim Biophys Acta*, 2010, **1802**, 322-330.
50. B. H. J. Bielski, G. G. Shiue and S. Bajuk, *The Journal of Physical Chemistry*, 1980, **84**, 830-833.
51. C. Chavarría and J. M. Souza, *Archives of Biochemistry and Biophysics*, 2013, **533**, 25-32.